Evolution of Species' Range and Niche in Changing Environments

Jitka Polechová[a]

[a]Department of Mathematics, University of Vienna, Oskar-Morgenstern Platz 1, A-1090 Vienna, Austria. E-mail: jitka@univie.ac.at

This manuscript was compiled on April 9, 2025

In times of accelerating climate change, there is an urgent need for a predictive theory of species' range shifts, adaptation, and species' resilience under changing environments. Current predictions are limited, as they rely on theory that neglects important interactions between ecological and evolutionary forces. Here, I show that the feedback between selection, genetic drift, and population dynamics fundamentally changes these predictions. This eco-evolutionary feedback creates a tipping point where genetic drift overwhelms selection, and species' range contracts from the margins or fragments abruptly – even under gradual environmental change. This tipping point is determined by three parameters: two quantifying the effects of spatial and temporal variability on fitness, and one capturing the impact of genetic drift. Importantly, I show that by increasing the "neighbourhood size", dispersal can counteract the loss of genetic variation, which would otherwise limit evolvability and increase extinction risk. This suggests that increasing local dispersal, possibly via assisted migration, can facilitate evolutionary rescue when local population size is small. While standard ecological niche models assume that species' ranges shift with environmental change, this study shows that eco-evolutionary feedback can lead to a sudden range fragmentation into disjunct subpopulations with depleted genetic variance, increasing the probability of extinction.

eco-evolutionary dynamics | gene flow | range margin | adaptation | ecological niche modelling

DRAFT

Introduction. As environments change over time, species' ranges may shift, expand, or contract, while their ecological niches change through adaptation. These evolutionary and ecological processes are interconnected: population growth is determined by the mean fitness of the population, while the rate of adaptation depends on the genetic variance, the strength of natural selection, and the genetic drift (1–3). Even considering a single focal species, the interaction between demographic and evolutionary dynamics in spatially and temporally varying environments is complex and difficult to predict. Theoretical progress has often relied on simplifying assumptions such as treating genetic variance as fixed (4–7) or neglecting two-dimensional spatial structure and modelling a small number of loci, particularly in evolutionary rescue models (8–10). In contrast, the ecological niche modelling (ENM) framework typically considers multidimensional niche space that includes both biotic and abiotic components but does not account for adaptive potential (11), with only recent advances incorporating adaptive genetic diversity (12, 13).

Adaptive genetic variance drives the rate of evolution while also evolving under eco-evolutionary feedback. Importantly, the effects of spatial and temporal variability interact, influencing adaptation rates and the probability of evolutionary rescue (14–21). In spatially structured populations, gene flow across heterogeneous environments maintains a substantial proportion of genetic variance: the relative contribution of mutation-selection balance diminishes with increasing environmental heterogeneity and dispersal. While the increase in genetic variance due to temporal variation is inherently transient, driven by recurrent sweeps of beneficial mutations (22), this variability can persist over longer time scales in spatially structured populations. Therefore, it is important to consider spatial and temporal variation jointly and to include the feedback between population and evolutionary dynamics, while accounting for genetic and demographic stochasticity in two-dimensional habitats. However, to date, we still lack analyses integrating all these components and their interactions. This study demonstrates that this complexity is essential for capturing the essence of the eco-evolutionary dynamics of a species' range and niche, and provides novel predictions.

One of the key factors influencing species' range dynamics and the resilience of populations facing rapid environmental change is dispersal (23, 24). A central concept in Wright's (25) shifting balance theory, population subdivision and dispersal play a complex role even on smooth fitness landscapes (26). Haldane (27) introduced the idea of a feedback between asymmetric gene flow and the reduction of local population size as a key driver of stable species' range margins – an example of migration meltdown (28) due to "swamping" gene flow. However, increased gene flow does not necessarily hinder adaptation to environmental gradients. As genetic variance increases due to gene flow across heterogenous environments (29, 30), it not only elevates the standing load (fitness cost of genetic variance) but also accelerates the rate of adaptation and reduces lag load – the fitness cost of the distance between a trait mean and its optimum (31)).

Dispersal also influences stochasticity as it enlarges neighbourhood size, thereby decreasing the power of genetic drift relative to selection. Defined by Wright (32, 33), neighbourhood size quantifies the strength of genetic drift in populations distributed across continuous space and corresponds to the population within one standard deviation of the dispersal distance σ. In two dimensions with diffusive dispersal, neighbourhood size is given by $\mathcal{N} = 2\pi\,\sigma^2\,N$, representing the population within a circular area of diameter σ and local density N – effectively a local mating pool. Interestingly, although a suffi-

ciently large neighbourhood size is critical for the maintenance of adaptive diversity across space (34–36), it is – unlike effective population size or census size – currently almost never explicitly considered in conservation guidelines [though see (37–39)]. Despite a growing understanding that higher dispersal and gene flow may enhance population resilience, especially under changing environments (40), the importance of population structure, and neighbourhood size in particular, remains neglected.

Model and methodology summary. The core features of the model are eco-evolutionary feedback through the coupling between fitness and population growth, the inclusion of both genetic and demographic stochasticity, and a quantitative genetic model in which both the trait mean and its variance evolve. The effect of environment (biotic and abiotic) is represented by a gradient in the optimum value of a trait of the focal species. The optimum changes through time along one spatial coordinate: an example could be a spatial gradient in optimal flowering time, changing with altitude (but not along the contours of a hill) and time. Both range and niche shifts are possible, as suitable habitats can be accessed through dispersal, while the selected trait – including its variance – evolves in response to environmental change.

Individual fitness depends on both the local density and distance of the trait from the environmental optimum. The population growth is given by the mean fitness, which reflects the local density and phenotypic distance from the optimum. Selection is hard (*sensu* (41)): i.e., the locally attainable density ("carrying capacity") declines with maladaptation. An additive quantitative trait that influences adaptation to the environment is determined by a large number of loci with exponentially distributed effects α_i. There is free recombination but there are no differences between sexes; for simplicity, individuals are assumed to be hermaphroditic and haploid. Thus, there are no dominance effects; yet there is epistasis as the fitness effect of each allele depends on other allele frequencies via the trait mean. The dispersal distances are normally distributed, independent of fitness and do not evolve through time. The model is written as both an individual-based discrete-time simulation and as an analytical continuous-time model of joint evolutionary and population dynamics.

The dynamics of this complex model is elucidated with the help of the following steps. First, the continuous-time model is rescaled in terms of dimensionless parameters. This reduces dimensions of the system, simplifies the analysis and facilitates the future testing of predictions. Second, the outcomes of the individual-based model are compared to known analytical expectations of simpler systems: namely to the deterministic equilibria and the predictions of a phenotypic model with fixed genetic variance. An illustrative example of the individual-based model is given at Fig. S1.

Results.

Scale-free parameters of the model. This model of species' range and niche dynamics has over ten parameters, which arise from coupling the classic formalizations of evolutionary and ecological dynamics. Fortunately, there is a rescaling which both reduces the apparent dimensionality of the problem and facilitates interpretation. Upon nondimensionalization, we obtain five dimensionless parameters that describe the core system (extending from (5, 42, 43)). The first parameter measures the effective rate of change of the optimum through time: $k^* = k/\sqrt{V_s\, r^{*3}}$ relative to the strength of stabilising selection V_s and the rate r^* at which the population returns to its demographic equilibrium, where k is the rate of temporal change. The second parameter $B = b\,\sigma/(\sqrt{2V_s}\, r^*)$ describes the effective steepness of the environmental gradient b across space x in terms of the expected reduction in fitness due to dispersal σ. The third parameter is the neighbourhood size $\mathcal{N} = 2\pi\,\sigma^2\,N$, which describes the population attainable within a generation's dispersal and measures the weakness of genetic drift on local scales; N is the local population density. (There is a 2 rather than 4 as the model is haploid – for a diploid organism, neighbourhood size doubles.) The fourth parameter is the strength of selection $s \equiv \alpha^2/V_s$ relative to the rate of return of population to a demographic equilibrium s/r^* and finally the fifth is the scaled mutation rate μ/r^*. Further details on the model and its scaling are provided in the Methods.

Known predictions: fixed variance or no temporal change. The rate of adaptation increases with the product of selection gradient and additive genetic variance (2, 44). The genetic variance itself increases with the effective environmental gradient B such that in the absence of stochastic and demographic effects, the scaled genetic variance is $A = V_G/(r^*\,V_s) = \sqrt{2}B$ (45). We might thus expect that with increasing heterogeneity of the environment, measured by the effective environmental gradient B, the genetic variance will steadily rise and thus support adaptation to ever-increasing temporal change k^*: yet, this would only be true in infinitely large populations. Increasing spatial heterogeneity aids adaptation until the load due to genetic variance becomes too large: eventually, the coupling between evolution and demography incurs a load high enough to drive the population to extinction. Furthermore, long before the deterministic extinction, genetic and demographic stochasticity reshape the dynamics.

The influence of the effective environmental gradient B and the effective rate of temporal change k^* on the rate of species' range and niche expansion is demonstrated in Fig. 1. It shows that there is a fundamental bound to species' range expansion at $k^*_{e,det} = \sqrt{2}A = 2B$ (red dashed line), which extends from the threshold derived by (31) for a given genetic variance in the absence of spatial structure. The depicted line uses the predicted deterministic genetic variance maintained by gene flow across heterogeneous environments. Yet, adaptation to temporal change fails considerably before this upper bound is reached. This is because genetic drift depletes genetic variance when neighbourhood size $\mathcal{N}$ is small, which hinders adaptation. In the absence of temporal change, the limit where continuous adaptation to environmental gradients is possible is given by $\mathcal{N} \gtrapprox 6.3\,B + 0.56$ (43). Below this limit, genetic drift is too strong relative to selection for stable clines to form. This threshold is depicted by a green diamond ♦ in Fig. 1.

Expansion threshold. When the optimum changes through time, the above limit to adaptation changes. A moving optimum induces a lag load. This demographic cost further lowers the

DRAFT

neighbourhood size and thus depletes genetic variance as genetic drift becomes stronger. The expansion threshold in changing environments is determined jointly by the effective environmental gradient B, the neighbourhood size $\mathcal{N}$ and the effective rate of temporal change k^*. Its approximate form, expressed for the critical effective rate of temporal change k_e^*, is given by $k_e^* = 2B\,(1 - 8/\mathcal{N})\sqrt{1 - (6.3B + 0.56)(\sqrt{2}B + 2h^2)/(2h^2\mathcal{N})}$, is shown by a green curve in Fig. 1; $h^2 \equiv V_G/V_P$ gives the narrow-sense heritability for the additive trait. Note that this approximate threshold, which marks the transition between expanding well-adapted populations with variance maintained by staggered clines in allele frequencies *vs.* collapsing populations where genetic drift overwhelms selection and the variance is depleted, only depends on the balance of k^*, B and $\mathcal{N}$. In contrast, rates of adaptation and range expansion also depend on the mutational input μ/r^* and the selection strength per locus, s/r^*. The robustness of the threshold to selection per locus $s \equiv \alpha^2/V_s$ is demonstrated in Fig. S3.

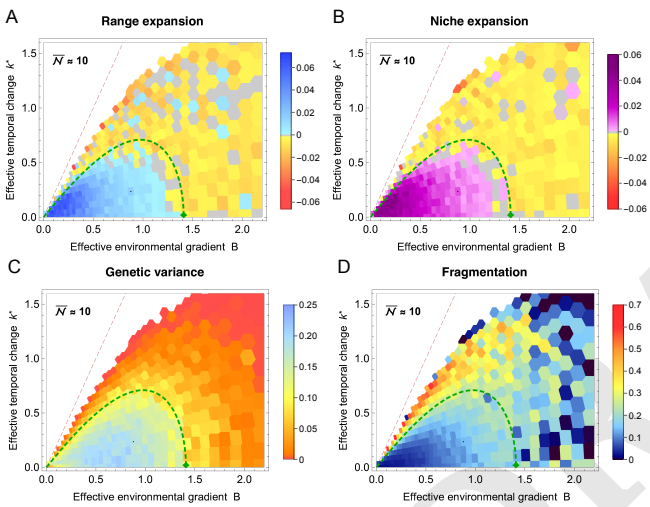

Fig. 1. Coevolution of species' range, niche and local genetic variance. Species' range and niche expand when sufficient variance is maintained by the gene flow across the environmental gradient and contract or fragment otherwise. Each rectangle represents an independent simulation from an array of changing environmental gradients b and rates of temporal change k. The expansion threshold is shown in a green dashed curve, approximated by $k_e^* = 2B\,(1 - 8/\mathcal{N})\sqrt{1 - (6.3B + 0.56)(\sqrt{2}B + 2h^2)/(2h^2\mathcal{N})}$. The deterministic extinction limit $k_{e,det}^* = 2B$ is depicted in a red dashed line. (A) The rate of range expansion relative to the initial range size is shown in blue, while the rate of niche expansion in (B) is shown in purple. The rates of range and niche contraction are shown in orange and red hues. Grey indicates no significant change (95% CI) and white space represents extinctions within 500 generations. (C) Genetic variance initially increases with both spatial and temporal variability but collapses abruptly at the expansion threshold where the effect of genetic drift overwhelms selection. (D) Species' range fragments abruptly as temporal change increases. Fragmentation is measured as the proportion of unoccupied space within the species' range. Fragmentation correlates with an increased probability of local extinction, resulting in high stochasticity in fragmentation on very steep gradients because fragmentation of the last subpopulation is zero. Median neighbourhood size $\overline{\mathcal{N}} = 2\pi\sigma^2 N \approx 10$ ranges between 8 and 17 (and is higher for lower B and k^*, where the overall demographic load is lower); median total population size is about $3.2 \cdot 10^3$ for all surviving populations, ranging from 450 for expanding populations to $3 \cdot 10^5$ at $T = 500$ generations. See Methods for parameters.

The prediction generalised expansion threshold utilises the expected increase of demographic loads due to k^* and B as well as the reduction of genetic variance due to genetic drift (yet is partly heuristic). In the absence of genetic drift, the tension between local adaptation and gene flow across heterogeneous environments leads to staggered clines, with local genetic variance of $V_{G,det} = b\,\sigma\sqrt{V_s} + V_m$ (45), where the mutational variance is $V_m = 2\mu\, n_l V_s$ and n_l denotes the number of loci. When genetic drift increases relative to selection, these clines will become increasingly rugged and move in position as well as steepen (34, 46, 47). The rugged allele frequencies may still contribute to adaptation even when they do not resemble a conventional cline (48, 49). There is no exact analytical expression for effect of genetic drift on a cline and thus genetic variance in two dimensional habitats but we can approximate the decrease of genetic variance with drift as $V_G \approx V_{G,det}(1 - 8/\mathcal{N})$ for $\mathcal{N} > 8$ – see Fig. 2. This estimate assumes that the reduction in genetic variance in two dimensions takes the same form as in one dimension (35), with the dimension-appropriate neighbourhood size, and the constant of 8 is numerically fitted. When the optimum changes both in time and space, the selection arising from the distance between the trait mean will favour clines in additional allele frequencies, which then shift through space. This drives an increase of genetic variance which is stable over longer time scales (relative to well-mixed populations (22)). More generally, Fig. 2 demonstrates that neighbourhood size, rather than total (effective) population size, fundamentally drives the increase of genetic variance. Quantitative analysis of the evolution of variance in both spatially and temporally variable environments will be the subject of a forthcoming paper.

Fragmentation. When the strength of genetic drift and the rate of temporal change are high, species' range may fragment abruptly: see Fig. 3. The example in Fig. 4 and Movie S1 illustrates that fragmentation can occur abruptly across the entire geographic range, and it is underlined by fragmentation in the trait (ecological niche) space and depleted genetic variance. Fragmentation occurs readily under rapid temporal change which generates a large lag load as trait mean lags behind the moving optimum. This is because there are two distinct modes in which a population can persist under a moving optimum: one includes adaptation while maintaining genetic variance, as well as range shift, and the other is by purely tracking the old optimum through space as long as it remains available (5). As the fitness load due to variance, lag and dispersal approaches the maximum intrinsic rate of increase, the population can only survive by tracking through space, while its variance and lag loads are low. However, this leads to population fragmentation and significantly reduced population resilience, as the population lacks adaptive variance and is subject to large demographic fluctuations. A larger neighbourhood size coupled with higher adaptive variance maintained by dispersal across heterogeneous environments prevents fragmentation unless rate of temporal change exceeds the expansion threshold k_e^* and approaches deterministic limit k_c^* (see Fig. 1 D). Note that a species' range can also fragment in the absence of temporal change when neighbourhood size is small (43). Due to strong genetic drift, clines in allele frequencies become increasingly rugged, steep and unstable. As clines steepen and variation in allele frequencies is lost, genetic variance is depleted and becomes too low to support a continuous adaptation (52, Fig. 4). In general, population fragments as genetic variance becomes depleted, which prevents continuous adaptation to spatially and temporally variable environments. Demographic fluctuations, while not a

DRAFT

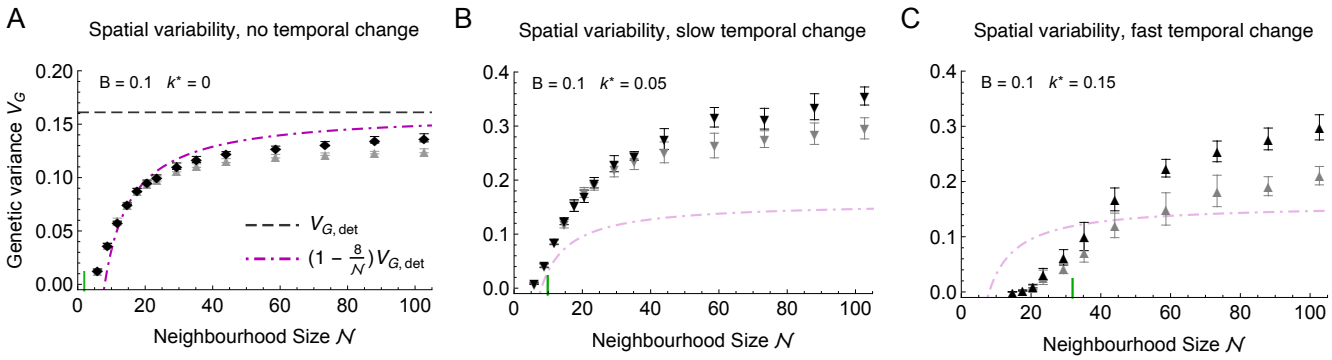

Fig. 2. Genetic variance is significantly reduced when neighbourhood size $\mathcal{N}$ is low. As the effective rate of temporal change k^* increases, larger neighbourhood size is necessary so that the population can sustain itself: the expansion threshold (in terms of $\mathcal{N}(k^*, B)$), illustrated by I, is roughly at the inflection point for the increase of genetic variance with $\mathcal{N}$. (A) In stable environments, the decrease in genetic variance due to drift in two-dimensional habitats approximately follows $V_G \approx V_{G,det}(1 - 8/\mathcal{N})$, shown as a dash-dotted magenta curve. Deterministic variance (dashed line) is given by $V_{G,det} = b\,\sigma\sqrt{V_s} + V_m$ (see text). (B) When the environment changes slowly through time (at $k^* \ll k_e^*$), genetic variance can increase substantially as newly selected alleles spread through the population.The increase of genetic variance with k^* is non-monotonic – with fast temporal change (C), increasing genetic drift suppresses the increase in variance. Black symbols: neutral habitat width is fixed at $y_d = 100$, so that total population increases with $\mathcal{N}$ and the habitat remains truly two-dimensional. Gray symbols represent simulations where neutral habitat width scales inversely with carrying capacity ($y_d = 600/K$), ensuring similar census sizes as $\mathcal{N}$ increases ($N_{tot} \approx 1.5 \cdot 10^5$). When the neutral habitat width y_d becomes too narrow due to scaling, genetic variance increases less than expected (gray, $y_d \lessapprox 50$ for $\mathcal{N} \gtrapprox 60$). This is largely because in the limit of a one-dimensional habitat ($y_d = 1$), the strength of genetic drift scales with $1/(\sqrt{s}\,\mathcal{N}_{1D})$ (35, 50, 51), where the one-dimensional neighbourhood size is $\mathcal{N}_{1D} = 2\sqrt{\pi}N\sigma$ (32). Error bars show standard deviations (10 replicates). Parameters as in Fig. 1 with $b = 0.225$, $k = 0$ (A), $k = 0.06 \equiv k^* = 0.05$ (B) and $k = 0.18 \equiv k^* = 0.15$ (C), run time $T = 300$ generations and neighbourhood size $\mathcal{N} = 2\pi\sigma^2 N \approx 2\pi\sigma^2 K(1 - B/\sqrt{2})$, where local carrying capacity ranges from $K = 2$ to $K = 35$.

primary driver, can further exacerbate the fragmentation and accelerate the population's collapse.

Dispersal and neighbourhood size. Larger neighbourhood size (the population accessible by dispersal) promotes adaptation by mitigating genetic drift and supporting adaptation to steeper environmental gradients B and faster temporal change k^*. Supplementary Figs. S4 and S5 show that the expansion threshold k_e^* decreases with neighbourhood size $\mathcal{N}$. Even when the total population size is kept approximately constant, adaptation fails sooner as neighbourhood size decreases (Fig. S4, $\overline{\mathcal{N}} = 8$ *vs.* Fig. S5, $\overline{\mathcal{N}} = 14$).

Neighbourhood size also increases with dispersal, but so does the effective environmental gradient B. However, in two dimensions, neighbourhood size $\mathcal{N} = 2\pi\sigma^2 N$ increases with the square of dispersal distance σ^2, while the effective gradient $B = b\,\sigma/(\sqrt{2V_s}\,r^*)$ increases only linearly. Therefore, increasing local dispersal aids adaptation when genetic drift is strong. Fig. S6 demonstrates that the benefits of reducing genetic drift *via* increased dispersal outweigh the costs associated with increasing dispersal load.

Adaptive phenotypic plasticity. Last, I briefly explore the effects of adaptive phenotypic plasticity. Fig. S7 demonstrates that adaptive phenotypic plasticity does not extend the range of survivable rates of temporal change in the same manner as it does for spatial variability. Adaptive phenotypic plasticity implies that the expressed trait z is closer to the optimum θ than expected based on its genetic basis alone, $(z - \theta) \to (1 - \mathfrak{p})\,(z - \theta)$, where $\mathfrak{p}$ denotes adaptive plasticity. This means that the spatial gradient B appears shallower by $1 - \mathfrak{p}$. While this reduces the demographic load and lowers the impact of genetic drift, it also diminishes the increase in genetic variance due to spatial variability. Thus, when genetic variance evolves in response to the effective environmental gradient, the effects of plasticity on adaptation to a steady temporal change largely cancel out. This finding contrasts with predictions assuming

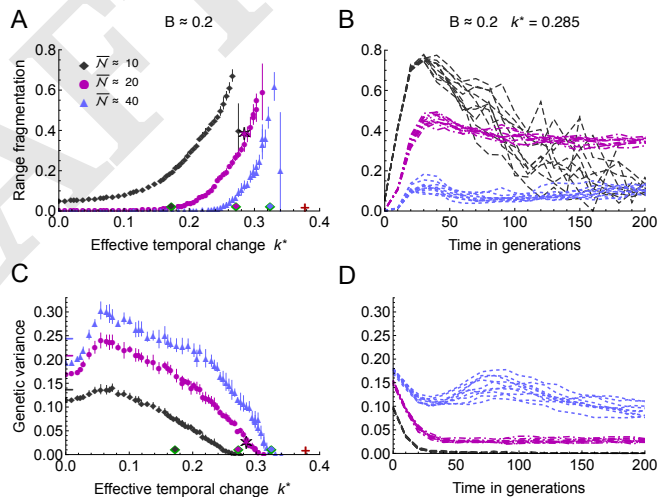

Fig. 3. Species' range fragments under rapid temporal change and small neighbourhood size. (A) Range fragmentation increases with the effective rate of temporal change k^* and decreasing neighbourhood size $\mathcal{N}$. The expansion threshold $k_e^*(B, \mathcal{N})$ is shown as green-outlined diamonds with coloured centres matching the respective neighbourhood sizes (and roughly corresponds to fragmentation above 0.2). The deterministic extinction threshold $k_{e,det}^* = 2B$ is marked with a red cross. (B) Beyond the expansion threshold, the onset of fragmentation is rapid and associated with a loss of genetic variance. The apparent decrease in fragmentation for $\mathcal{N} \approx 10$ is due to only a few fragments remaining in fast-collapsing populations. (C) Genetic variance decreases with genetic drift (i.e., decreasing neighbourhood size $\mathcal{N}$) and is highest for intermediate rates of temporal change before declining again. Dashes at $k^* = 0$ represent the predicted genetic variance in stable environments, accounting for genetic drift. (D) Genetic variance drops as populations fragment when neighbourhood size is small. Only for $\mathcal{N} = 20$ (above the expansion threshold), there is a temporary recovery, as selection due to the lag of the trait mean behind the optimum drives further clines which elevate genetic variance – before variance stabilizes at about $V_G = 0.1$. Parameters as in Fig. 1 with $b = 0.4$ and $k = 0.31 \equiv k^* = 0.285$ for (C, D); the magenta star marks an illustration shown in Fig. 4. Neighbourhood sizes are slightly below the maximum attainable neighbourhood size $\mathcal{N} = 2\pi\sigma^2 K$ and correspond to local carrying capacities $K = 5, 10, 20$.

DRAFT

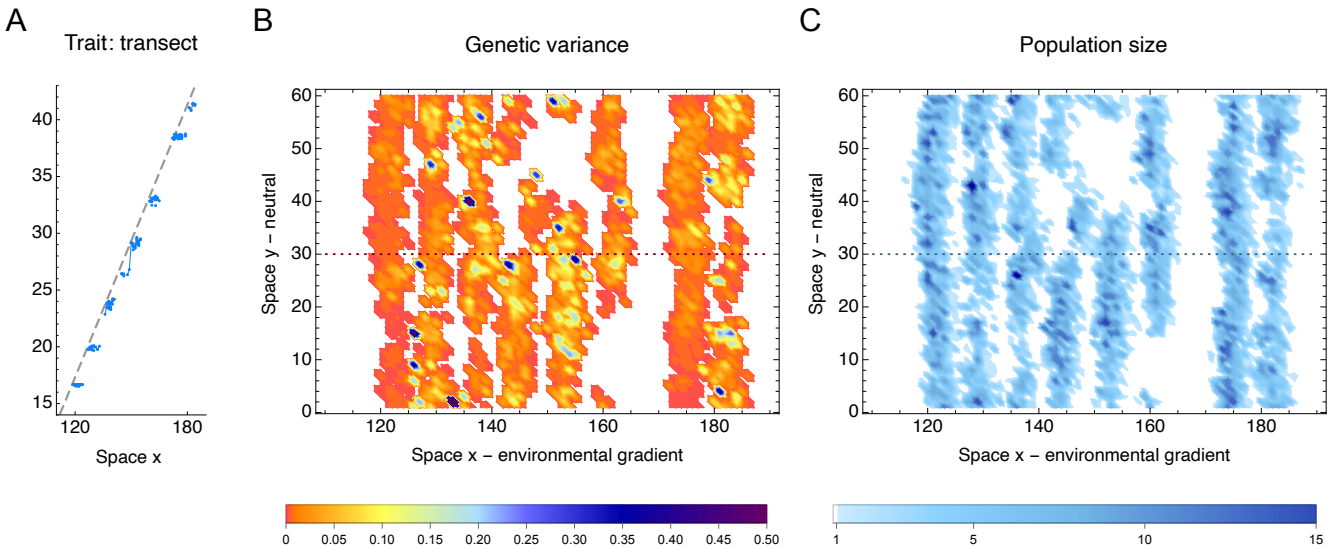

Fig. 4. Example of species' range fragmentation due to a fast temporal change. (A) In fragmented populations, trait mean (blue line) no longer tracks the optimum (grey dashed line) but instead, disjunct subpopulations are each adapted to a single optimum and move through space tracking their niche. Blue dots show individual trait values. The subfigure (A) shows a transect at the central neutral habitat ($y = 30$), marked by the dotted line in (B, C). (B) Genetic variance is depleted considerably below the expected value of $V_G \approx (b\,\sigma\sqrt{V_s} + V_m)(1 - 8/\mathcal{N}) = 0.21$, although local spikes of high variance (blue hues) persist. (C) Local population size is close to the carrying capacity $K = 10$, yet 40% of the space is unoccupied, and the population gradually contracts over time. Subpopulations are connected *via* gene flow along the neutral habitat (y) but largely isolated along the environmental gradient (x). Parameters are the same as in Fig. 3 (K = 10, magenta), with $k^* = 0.285$, indicated by magenta star there. This example is chosen just beyond the expansion threshold $k_e^*(B, \mathcal{N}) \approx 0.273$, where some clines in allele frequencies still persist and therefore variance is not uniformly low. The dynamics of fragmentation is illustrated in Supplementary Movie S1, demonstrating that fragmentation occurs abruptly and follows a marked increase in lag (and thus lag load) behind the moving optimum.

fixed genetic variance in the selected trait, where the benefits of plasticity in response to variation in time and space are equivalent (6, 53).

Discussion. There is an urgent need for predictive theory to forecast adaptive responses and population resilience in changing environments (14, 54, 55). While phenotypic models provide a useful reference (6, 7), the absence of evolutionary genetics not only precludes any inference based on genetic data but also weakens the reliability of predictions. Both the effects of gene flow and the possible benefits of adaptive plasticity change fundamentally when population genetics is included (43, 56). Adaptation typically involves changes across many loci, and predicting the trajectory of each of them is not feasible (57). In contrast, predictions based on higher-order parameters derived from fundamental population genetics (such as additive variance in the selected trait) tend to be robust (58, 59).

This theory provides quantitative predictions concerning species' range limits, adaptation, and resilience. It explains that a gradual increase in the rate of temporal change, as well as a decrease in neighbourhood size $\mathcal{N}$, can lead to a tipping point where adaptation collapses. Neighbourhood size, the population accessible by dispersal within a generation, can decline due to limited dispersal (e.g. reduced connectivity) or a decrease in local population density. Beyond this eco-evolutionary tipping point, genetic drift becomes too strong relative to the strength of environmental change, leading to the collapse of clinal adaptation. The population may decline gradually, with the species' range contracting from the margins, or fragment abruptly. While fragmentation due to spatial variation alone is limited to low neighbourhood sizes (43), when the loss of fitness maladaptation induced by temporal change is high, fragmentation can occur rapidly even when genetic drift is not particularly strong. Since fragmentation is associated with a loss of genetic variance in the selected traits as well as increased demographic stochasticity, recovery is likely to be hindered even if conditions later improve.

Importantly, the predictive parameters are measurable: thus, the theory can be tested and offers applications in conservation genetics. Neighbourhood size $\mathcal{N}$ can be estimated from ecological parameters of local density and dispersal as well as from population-genetic parameters – specifically, the rate of increase in neutral F_{ST} with distance (60, Eq. 11). However, F_{ST} will be affected by population dynamics: see (38, 61) for estimates and discussion of assumptions. Demographic load parameters B and k^* quantify fitness loss due to spatial and temporal environmental variability. The dispersal load can be estimated from transplant experiments: moving a well-adapted population by a distance σ reduces fitness by $B^2 r^{*2}$. The fitness cost of temporal change $k^{*2} r^*/2$, over a characteristic time $1/r^*$, is more challenging to infer: in some cases, past generations' fitness can be assessed using seeds or diapausing animals, or more commonly, by substituting space for time (62, 63) in spatial transplant experiments – see (5, Discussion).

There are three major limitations to this theory. First, it considers a single trait under stabilising selection assuming no rigid genetic trade-off, which could further limit adaptation (64). Second, it considers gradual change in continuous environments. In reality, the environment may be patchy and selection fluctuates through time, with extremes potentially

DRAFT

incurring higher fitness costs than the steady change. Each of these complications are likely to hinder adaptation (65, 66). Third, the theory considers a single focal species. Although the environmental optimum can include both abiotic and biotic components (67), the theory neglects the co-evolution of species over similar time scales (68, 69). While none of these concerns invalidate the scale-free parameters, they imply that the numerical value of the expansion threshold should be considered an approximate baseline, rather than a definitive value.

The theory shows that when dispersal is predominantly local (diffusive), eco-evolutionary dynamics is determined over local scales. A minor proportion of long-distance dispersers does not substantially change the predictions [see (70) in the absence of temporal change]. Therefore, the theory does not require spatial gradients to be linear; it also applies to other forms of gradual change, such as steepening gradients (43, 71–73). Because the dynamics is local and the predicted range margin is abrupt, the theory makes no claims about the abundant center of a species' range (74, 75).

Conservation genetics has been increasingly incorporated into conservation practice, and a decline in heterozygosity or effective population size N_e would be a clear cause for concern (76). Yet, the utility of any cut-off value for effective population size N_e remains contested (77–80). At the same time, assisted migration (40, 81) is increasingly advocated as a strategy to facilitate adaptation under climate change. Until now, no comprehensive predictive theory has incorporated the effects of gene flow across variable environments on local polygenic adaptation and species' range dynamics under temporal change. This theory provides a foundation for predicting when an increase in local dispersal is likely to be beneficial and identifies a critical threshold beyond which the population may be at risk of collapse or abrupt fragmentation.

Materials and Methods

The model is of evolution of a species' range in two dimensions, where both population dynamics and evolution (at many additive loci) are considered jointly. The eco-evo coupling occurs through the mean fitness $\overline{r}(\overline{z}, N)$, which gives the growth rate of the population, decreasing with maladaptation: $\overline{r}(\overline{z}, N) = r_e(N) + \overline{r}_g(\overline{z})$. The ecological component of growth rate, r_e, can take various forms. Here, we assume logistic regulation, so that fitness declines linearly with density N: $r_e = r_m(1 - N/K)$, where r_m is the maximum per capita growth rate in the limit of the local population density $N \to 0$. The maximum carrying capacity K is assumed to be uniform across space. The second term, $r_g(\overline{z}) \leq 0$, represents the reduction in growth rate due to deviation from the optimum.
Selection is stabilising: the optimum $\theta = b\,x - k\,t$ changes smoothly (with a gradient b) along one spatial dimension (x), and through time t at a constant rate k. For any individual with a trait value of z, the drop in fitness due to maladaptation is $r_g(z) = -(z-\theta)^2/(2V_s)$, where $1/V_s$ gives the strength of stabilising selection. A population with a mean phenotype $\overline{z}$ has its fitness reduced by $\overline{r}_g(\overline{z}) = -(\overline{z}-\theta)^2/(2V_s) - V_P/(2V_s)$. The phenotype z is determined by many di-allelic loci with allelic effects α_i; the model is haploid, hence $\overline{z} = \sum_i \alpha_i p_i$, where p_i is the allele frequency at locus i. Phenotypic variance is $V_P = V_G + V_E$. The loss of fitness due to environmental variance V_E can be included in $r_m^* = r_m - V_E/(2V_s)$; V_E is a redundant parameter (and thus is set to zero throughout). Selection is *hard*: both the mean fitness (growth rate) and the attainable equilibrium density $\hat{N} = Kr^*/r_m = K(1 - V_P/(2r_m V_s))$ decrease as maladaptation increases. In the absence of genetic drift and no temporal change, genetic variance is largely maintained by gene flow: $V_G \approx b\,\sigma\sqrt{V_s}$ (45) and the contribution of mutation is relatively small.

Evolution of trait mean with joint population dynamics; unscaled. For any given additive genetic variance V_G (assuming a Gaussian distribution of breeding values), the change in the trait mean $\overline{z}$ over time satisfies:

$$\frac{\partial \overline{z}}{\partial t} = \frac{\sigma^2}{2}\left(\frac{\partial^2 \overline{z}}{\partial x^2} + \frac{\partial^2 \overline{z}}{\partial y^2}\right) + \sigma^2\left(\frac{\partial^2 \ln(N)}{\partial x}\frac{\partial \overline{z}}{\partial x} + \frac{\partial^2 \ln(N)}{\partial y}\frac{\partial \overline{z}}{\partial y}\right) + V_G\frac{\partial \overline{r}}{\partial \overline{z}} + \zeta \qquad [1]$$

The first term gives the change in the trait mean due to migration, with a mean displacement of σ; the second term describes the effect of the asymmetric flow from areas of higher density. The third term gives the change due to selection, given by the product of genetic variance and gradient in mean fitness (4, Eq. 2). The last term ζ gives the fluctuations in the trait variance due to genetic drift: $\zeta = \sqrt{V_{G,LE}/N}\,dW_\zeta(x,y,t)$, where dW_* represents white noise in space and time (34, 82). $V_{G,LE} = \sum_i \alpha_i^2 p_i q_i$ denotes genetic variance assuming linkage equilibrium. Note that the diffusion approximation breaks down over very local scales in two dimensions because in a continuous two-dimensional habitat, two independent Brownian motions will, with probability one, never be in the same place at the same time (and thus, there would be no coalescence). The simulation avoids this problem by considering a discrete lattice, an analytical approach would require the introduction of a local scale of population interactions (82).

The trait mean is $\overline{z} = \sum_i \alpha_i p_i$ for a haploid model, where p_i is the i-th allele frequency, $q_i = 1 - p_i$ and α_i is the effect of the allele on the trait – the change of the trait mean $\overline{z}$ as frequency of locus i changes from 0 to 1. For both haploid and diploid models, the allele frequencies p_i change as:

$$\begin{aligned}\frac{\partial p_i}{\partial t} &= \frac{\sigma^2}{2}\left(\frac{\partial^2 p_i}{\partial x^2} + \frac{\partial^2 p_i}{\partial y^2}\right) + \sigma^2\left(\frac{\partial p_i}{\partial x}\frac{\partial \ln(N)}{\partial x} + \frac{\partial p_i}{\partial y}\frac{\partial \ln(N)}{\partial y}\right) + \\ &+ p_i q_i \frac{\partial \overline{r}}{\partial p_i} - \mu(p_i - q_i) + \epsilon \qquad [2]\end{aligned}$$

The expected change of allele frequency due to a gradient in fitness and local heterozygosity is $p_i q_i \frac{\partial \overline{r}}{\partial p_i} = s_i\, p_i q_i (p_i - q_i - 2\Delta_i)$, where selection at locus i is $s_i \equiv \alpha_i^2/(2V_s)$ and $\Delta_i = (\overline{z} - bx)/\alpha_i$ (45, Appendix 3). Here, the fourth term describes the change due to (symmetric) mutation at rate μ. The last term ϵ describes genetic drift (82, Eq. 7): $\epsilon = \sqrt{\frac{p_i q_i}{N}}\,dW_\epsilon(x,y,t)$; where N is the haploid population density.

Population dynamics reflect diffusive migration in two dimensions, growth due to the mean Malthusian fitness $\overline{r}$, and stochastic fluctuations. The number of offspring follows a Poisson distribution with mean and variance of N, fluctuations in population numbers are given by (83): $\xi = \sqrt{N}\,dW_\xi(x,y,t)$:

$$\frac{\partial N}{\partial t} = \frac{\sigma^2}{2}\left(\frac{\partial^2 N}{\partial x^2} + \frac{\partial^2 N}{\partial y^2}\right) + \overline{r}N + \xi \qquad [3]$$

Rescaling and formalising in terms of allele frequencies, with evolution of variance. The model can be simplified by rescaling time t relative to the strength of density dependence r^*, distance x relative to dispersal σ, trait z relative to strength of stabilising selection $1/(2V_s)$ and local population size N relative to equilibrium population size with perfect adaptation: $\hat{N} = Kr^*/r_m$, $T = r^*t$, $X = x\sqrt{\frac{2r^*}{\sigma^2}}$, $Z = \frac{z}{\sqrt{r^* V_s}}$, $\tilde{N} = N/\hat{N}$. Note that near the equilibrium of a well-adapted population, $\tilde{N} \approx 1$.

Assuming linkage equilibrium, the rescaled equations for evolution

DRAFT

of allele frequencies and for demographic dynamics are:

$$\begin{aligned}
\frac{\partial \tilde{N}}{\partial T} &= \frac{\partial^2 \tilde{N}}{\partial X^2} + \frac{\partial^2 \tilde{N}}{\partial Y^2} + \overline{R}\tilde{N} + \sqrt{\frac{2\tilde{N}}{\tilde{N}\sigma^2}}\, dW_{\tilde{\xi}(X,Y,T)} \\
\frac{\partial p_i}{\partial T} &= \frac{\partial^2 p_i}{\partial X^2} + \frac{\partial^2 p_i}{\partial Y^2} + 2(\frac{\partial p_i}{\partial X}\frac{\partial \ln(\tilde{N})}{\partial X} + \frac{\partial p_i}{\partial Y}\frac{\partial \ln(\tilde{N})}{\partial Y}) + \\
&+ \frac{s}{r^*}(p_i q_i - 2\frac{\overline{Z} - BX - k^*T}{\alpha^*}) - \frac{\mu}{r^*}(p_i - q_i) + \\
&+ \sqrt{\frac{pq}{\tilde{N}\hat{N}\sigma^2}}\, dW_{\tilde{\epsilon}(X,Y,T)} \qquad [4]
\end{aligned}$$

where

$$\overline{R} \equiv \overline{r}/r^* = 1 - \tilde{N} - (BX - k^*T - Z)^2/2. \qquad [5]$$

The rescaled equations 4 and 5 show that four parameters fully describe the system. First, the effective rate of temporal change, $k^* = k/\sqrt{V_s\, r^{*3}}$. Second, the effective environmental gradient, $B \equiv b\sigma/(r^*\sqrt{2V_s})$. Third, the strength of genetic drift $1/\hat{\mathcal{N}} = 1/(2\pi\hat{N}\sigma^2)$. The parameter $\hat{\mathcal{N}}$ gives the neighbourhood size of a well-adapted population at equilibrium. The fourth parameter is the strength of selection relative to the strength of density dependence, s/r^*; the scaled effect of a single substitution α^* also scales with s/r^*: $\alpha^* \equiv \alpha/\sqrt{r^* V_s} = \sqrt{2s/r^*}$. The effect of this fourth parameter s/r^* is expected to be small, because typically, $s \lll r^*$. The fifth parameter, μ/r^*, will typically be very small, and will be neglected throughout. Table 1 (top) summarises the full set that describes the system.

Table 1. Five scale-free parameters: B, k^*, $\mathcal{N}$, $s/r^*$and μ/r^* describe the system. Middle section gives informative derived parameters. The fifth parameter, scaled mutation rate μ/r^*, can be neglected because variance maintained by mutation-selection balance, $V_{G,\mu/s} = 2\mu V_s n_l$, is typically much smaller than variance generated by gene flow across environments, $V_G = b\,\sigma\sqrt{V_s}$. The middle column gives the dimensions of the parameters, where T stands for time, D for distance and Z for trait.

param.	dim.	description
k^*	–	effective rate of temporal change $k^* = k/\sqrt{V_s\, r^{*3}}$
B	–	effective environmental gradient $B = b\sigma/(r^*\sqrt{2V_s})$
$\mathcal{N}$	–	neighbourhood size $\mathcal{N} = 4\pi N_e\sigma^2 = 2\pi N\sigma^2$
s/r^*	–	strength of selection per locus relative to the strength of density-dependence
s	$1/T$	selection per locus: $s \equiv \alpha^2/(2V_s)$
r^*	$1/T$	rate of return to equilibrium pop. size: $r^* \equiv -N\,\partial\overline{r}/\partial N\|_{N\to\hat{N}} = r_m - V_G/(2V_s)$
b	Z/D	gradient in the environmental optimum
V_s	Z^2T	variance of stabilising selection
σ	$D/\sqrt{T}$	dispersal per generation
K	T/D^2	max. carrying capacity (haploid) K = N when all phenotypes are perfectly adapted
r_m	$1/T$	max. intrinsic rate of increase
α	Z	allelic effect
μ	$1/T$	mutation rate, $\mu \equiv 10^{-5}$

Individual-based simulations. Discrete-time individual based simulations are set to correspond to the model with continuous time and space. The life cycle is selection → mutation → recombination → birth → migration. Generations are non-overlapping and selfing is allowed at no cost. Every generation, each individual mates with a partner drawn from the same deme, with probability proportional to its fitness, to produce a number of offspring drawn from a Poisson distribution with mean of $Exp[r(z,N)]$. The effective diploid population density N_e hence equals half of the haploid population density N, and $\mathcal{N} = 4\pi N_e\sigma^2 = 2\pi N\sigma^2$.

The genome is haploid with 1000 unlinked loci, so the probability of recombination between any two loci is 1/2. The additive trait is determined by the sum of allelic effects α_i – they are exponentially distributed with mean of $\alpha = 0.07$ unless stated otherwise. This gives the mean strength of selection per locus $s = \alpha^2/(2V_s) \approx 0.005$. Mutation is set to $\mu = 10^{-5}$. Migration is diffusive with a Gaussian dispersal kernel. Due to the discretisation of the space, the tails of the dispersal kernel need to be truncated: truncation is set to three standard deviations of the dispersal kernel throughout, and dispersal probabilities and variance are adjusted so that the discretised dispersal kernel sums to 1 (84, p. 1209). The space is a two-dimensional lattice with spacing between demes of $\delta x = 1$, wide enough along both spatial dimensions x_d and y_d so that species' range does not reach the edges along the dimension of spatial change and that the random processes (genetic drift) occur in a truly two-dimensional habitat. Burn-in time (no temporal change) is 200 generations; run time 500 generations (unless stated otherwise). Simulations were written in Mathematica (Wolfram) and executed on the Vienna Scientific Cluster (VSC); the code will be available on Dryad upon acceptance.

Parameters (unless stated otherwise): dispersal per generation $\sigma^2 = 1/2$, width of stabilising selection $V_s = 1$, maximum growth rate $r_m = 1.2$, maximum local carrying capacity $K = 6$, mutation rate $\mu = 10^{-5}$, number of loci $n_l = 1000$. Initially, 1/3 of all loci form clines that contribute to the adaptation to the environmental gradient so that in the central part of the range, trait mean matches the environmental optimum. Allelic effects are exponentially distributed with mean $\alpha = 0.07$. The habitat is wide enough ($x_d \geq 600$) so that species' range does not reach the edges along the dimension of spatial change and that the random processes (genetic drift) occur in truly two-dimensional habitat: along the neutral dimension, the number of demes is $y_d = 600/K = 100$.

Acknowledgements. I would like to thank Nick Barton, Roger Butlin and Richard Nichols for discussions and detailed comments on earlier drafts, and Stuart Baird, Andrea Betancourt, Louise Fouqueau, Jan Hrček, Patrik Nosil, Pavel Payne and Jason Sexton for their comments on the manuscript. **Funding:** This research was funded by the Austrian Science Fund (FWF), project doi: 10.55776/P32896, Institutional Identifier: 501100002428, grant number P32896. The computational results were achieved using the Vienna Scientific Cluster (VSC).
For open access purposes, the author has applied a CC BY public copyright license to any author-accepted manuscript version arising from this submission.

Supplementary Materials. Supplementary Figures S1 to S7 with Legends
Supplementary Movie S1

References.

1. Haldane JBS (1957) The cost of natural selection. *Journal of Genetics* 55(3):511–524.
2. Lande R (1976) Natural selection and random genetic drift in phenotypic evolution. *Evolution* 30(2):314–334.
3. Paixão T, Barton NH (2016) The effect of gene interactions on the long-term response to selection. *Proceedings of the National Academy of Sciences* 113(16):4422–4427.
4. Pease C, Lande R, Bull J (1989) A model of population growth, dispersal and evolution in a changing environment. *Ecology* 70(6):1657–1664.
5. Polechová J, Barton N, Marion G (2009) Species' range: Adaptation in space and time. *The American Naturalist* 174(5):E186–204.
6. Chevin LM, Lande R, Mace GM (2010) Adaptation, plasticity, and extinction in a changing environment: towards a predictive theory. *PLoS Biology* 8(4):e1000357.
7. Aguilée R, Raoul G, Rousset F, Ronce O (2016) Pollen dispersal slows geographical range shift and accelerates ecological niche shift under climate change. *Proceedings of the National Academy of Sciences* 113(39):E5741–E5748.
8. Gomulkiewicz R, Holt RD (1995) When does evolution by natural selection prevent extinction? *Evolution* pp. 201–207.
9. Uecker H, Otto SP, Hermisson J (2014) Evolutionary rescue in structured populations. *The American Naturalist* 183(1):E17–E35.
10. Czuppon P, Blanquart F, Uecker H, Débarre F (2021) The effect of habitat choice on evolutionary rescue in subdivided populations. *The American Naturalist* 197(6):625–643.

DRAFT

11. Burrows MT, et al. (2014) Geographical limits to species-range shifts are suggested by climate velocity. *Nature* 507(7493):492–495.
12. Razgour O, et al. (2019) Considering adaptive genetic variation in climate change vulnerability assessment reduces species range loss projections. *Proceedings of the National Academy of Sciences* 116(21):10418–10423.
13. Thuiller W (2024) Ecological niche modelling. *Current Biology* 34(6):R225–R229.
14. Atkins K, Travis J (2010) Local adaptation and the evolution of species' ranges under climate change. *Journal of Theoretical Biology* 266(3):449–457.
15. Holt RD, Barfield M, Gomulkiewicz R (2004) Temporal variation can facilitate niche evolution in harsh sink environments. *The American Naturalist* 164(2):187–200.
16. Holt RD, Barfield M, Peniston JH (2022) Temporal variation may have diverse impacts on range limits. *Philosophical Transactions of the Royal Society B* 377(1848):20210016.
17. Sexton J, McIntyre P, Angert A, Rice K (2009) Evolution and ecology of species range limits. *Annual Review of Ecology, Evolution, and Systematics* 40:415–436.
18. Osmond MM, Klausmeier CA (2017) An evolutionary tipping point in a changing environment. *Evolution* 71(12):2930–2941.
19. Benning JW, Hufbauer RA, Weiss-Lehman C (2022) Increasing temporal variance leads to stable species range limits. *Proceedings of the Royal Society B* 289(1974):20220202.
20. Fouqueau L, Polechová J (2024) Eco-evolutionary dynamics in changing environments: integrating theory with data. *Journal of Evolutionary Biology* 37(6):579–587.
21. Tomasini M, Peischl S (2022) The role of spatial structure in multi-deme models of evolutionary rescue. *Journal of evolutionary biology* 35(7):986–1001.
22. Bürger R (1999) Evolution of genetic variability and the advantage of sex and recombination in changing environments. *Genetics* 153(2):1055–1069.
23. Holt RD, Gomulkiewicz R (1997) How does immigration influence local adaptation? a reexamination of a familiar paradigm. *The American Naturalist* 149(3):563–572.
24. Débarre F, Ronce O, Gandon S (2013) Quantifying the effects of migration and mutation on adaptation and demography in spatially heterogeneous environments. *Journal of Evolutionary Biology* 26(6):1185–1202.
25. Wright S, , et al. (1932) The roles of mutation, inbreeding, crossbreeding, and selection in evolution. *Proceedings of the 6th International Congress of Genetics* 1:356–366.
26. Garant D, Forde SE, Hendry AP (2007) The multifarious effects of dispersal and gene flow on contemporary adaptation. *Functional Ecology* 21(3):434–443.
27. Haldane JBS (1956) The relation between density regulation and natural selection. *Proceedings of the Royal Society of London, B: Biological Sciences* 145(920):306–308.
28. Ronce O, Kirkpatrick M (2001) When sources become sinks: migrational meldown in heterogeneous habitats. *Evolution* 55(8):1520–1531.
29. Felsenstein J (1976) The theoretical population genetics of variable selection and migration. *Annual review of genetics* 10(1):253–280.
30. Hedrick PW (1986) Genetic polymorphism in heterogeneous environments: a decade later. *Annual review of ecology and systematics* pp. 535–566.
31. Lande R, Shannon S (1996) The role of genetic variation in adaptation and population persistence in a changing environment. *Evolution* 50(1):434–437.
32. Wright S (1943) Isolation by distance. *Genetics* 28(2):114 – 138.
33. Wright S (1946) Isolation by distance under diverse systems of mating. *Genetics* 31(1):39.
34. Nagylaki T (1978) Random genetic drift in a cline. *Proceedings of the National Academy of Sciences of the United States of America* 75(1):423–426.
35. Polechová J, Barton N (2011) Genetic drift widens the expected cline but narrows the expected cline width. *Genetics* 1(189):227–235.
36. Charlesworth B, Charlesworth D, Barton NH (2003) The effects of genetic and geographic structure on neutral variation. *Annual Review of Ecology, Evolution, and Systematics* 34(1):99–125.
37. Lande R, Barrowclough GF, , et al. (1987) Effective population size, genetic variation, and their use in population management in *Viable populations for conservation*, ed. Soulé ME. (Cambridge University Press, Cambridge, UK), pp. 87–124.
38. Vekemans X, Hardy OJ (2004) New insights from fine-scale spatial genetic structure analyses in plant populations. *Molecular ecology* 13(4):921–935.
39. Richardson JL, Urban MC, Bolnick DI, Skelly DK (2014) Microgeographic adaptation and the spatial scale of evolution. *Trends in ecology & evolution* 29(3):165–176.
40. Sexton J, Clemens M, Hall J, Hoffmann A (2024) Patterns and effects of gene flow on adaptation across spatial scales: implications for management and models. *Journal of Evolutionary Biology* 37(6):732–745.
41. Christiansen FB (1975) Hard and soft selection in a subdivided population. *American Naturalist* 109(965):11–16.
42. Kirkpatrick M, Barton N (1997) Evolution of a species' range. *The American Naturalist* 150(1):1–23.
43. Polechová J (2018) Is the sky the limit? On the expansion threshold of a species' range. *PLoS Biology* 16(6):e2005372.
44. Fisher R (1930) *The genetical theory of natural selection*. (Clarendon Press, Oxford).
45. Barton N (2001) Adaptation at the edge of a species' range in *Integrating ecology and evolution in a spatial context*, 14th Special Symposium of the British Ecological Society, eds. Silvertown J, Antonovics J. (Cambridge University Press, Cambridge, UK), pp. 365–392.
46. Slatkin M, Maruyama T (1975) Genetic drift in a cline. *Genetics* 81(1):209–222.
47. Felsenstein J (1975) Genetic drift in clines which are maintained by migration and natural selection. *Genetics* 81(1):191–207.
48. Lotterhos KE (2023) The paradox of adaptive trait clines with nonclinal patterns in the underlying genes. *Proceedings of the National Academy of Sciences* 120(12):e2220313120.
49. Barton N (2024) Limits to species' range: the tension between local and global adaptation. *Journal of Evolutionary Biology* p. voae052.
50. Nagylaki T (1978) A diffusion model for geographically structured populations. *Journal of Mathematical Biology* 6(4):375–382.
51. Polechová J, Barton N (2015) Limits to adaptation along environmental gradients. *Proceedings of the National Academy of Sciences of the United States of America* 112(20):6401–6406.
52. Polechová J, Barton N (2015) Limits to adaptation along environmental gradients. *Proceedings of the National Academy of Sciences of the United States of America* 112(20):6401–6406.
53. King JG, Hadfield JD (2019) The evolution of phenotypic plasticity when environments fluctuate in time and space. *Evolution letters* 3(1):15–27.
54. Nadeau CP, Urban MC (2019) Eco-evolution on the edge during climate change. *Ecography* 42(7):1280–1297.
55. Urban MC, et al. (2024) When and how can we predict adaptive responses to climate change? *Evolution Letters* 8(1):172–187.
56. Whitlock MC (1996) The red queen beats the jack-of-all-trades: the limitations on the evolution of phenotypic plasticity and niche breadth. *The American Naturalist* 148:S65–S77.
57. Rudman SM, et al. (2022) Direct observation of adaptive tracking on ecological time scales in drosophila. *Science* 375(6586):eabj7484.
58. Barton N, Keightley P (2002) Understanding quantitative genetic variation. *Nature reviews genetics* 3(1):11–21.
59. Yang J, et al. (2010) Common snps explain a large proportion of the heritability for human height. *Nature genetics* 42(7):565–569.
60. Rousset F (1997) Genetic differentiation and estimation of gene flow from f-statistics under isolation by distance. *Genetics* 145(4):1219–1228.
61. Alberto F, et al. (2005) Within-population spatial genetic structure, neighbourhood size and clonal subrange in the seagrass *Cymodocea nodosa*. *Molecular Ecology* 14(9):2669–2681.
62. Blois JL, Williams JW, Fitzpatrick MC, Jackson ST, Ferrier S (2013) Space can substitute for time in predicting climate-change effects on biodiversity. *Proceedings of the national academy of sciences* 110(23):9374–9379.
63. Garcia Castillo D, et al. (2024) Predicting rapid adaptation in time from adaptation in space: a 30-year field experiment in marine snails. *Science Advances* 10(41):eadp2102.
64. Heblack J, Schepers JR, Willi Y (2024) Reduced evolutionary potential under heat and drought stress at the southern range edge of north american *Arabidopsis lyrata*. *Journal of Evolutionary Biology* p. voae045.
65. Botero CA, Weissing FJ, Wright J, Rubenstein DR (2015) Evolutionary tipping points in the capacity to adapt to environmental change. *Proceedings of the National Academy of Sciences* 112(1):184–189.
66. Gilbert KJ, Whitlock MC (2017) The genetics of adaptation to discrete heterogeneous environments: frequent mutation or large-effect alleles can allow range expansion. *Journal of evolutionary biology* 30(3):591–602.
67. Case T, Taper M (2000) Interspecific competition, environmental gradients, gene flow, and the coevolution of species' borders. *The American Naturalist* 155(5):583–605.
68. Long ZT, Petchey OL, Holt RD (2007) The effects of immigration and environmental variability on the persistence of an inferior competitor. *Ecology letters* 10(7):574–585.
69. Bridle J, Hoffmann A (2022) Understanding the biology of species' ranges: when and how does evolution change the rules of ecological engagement? *Philosophical Transactions of the Royal Society B* 377(1848):20210027.
70. Polechová J (2022) The costs and benefits of dispersal in small populations. *Philosophical Transactions of the Royal Society B* 377(1848):20210011.
71. Connallon T, Sgrò CM (2018) In search of a general theory of species' range evolution. *PLoS Biology* 16(6):e2006735.
72. Bridle JR, Kawata M, Butlin RK (2019) Local adaptation stops where ecological gradients steepen or are interrupted. *Evolutionary Applications* 12(7):1449–1462.
73. Angert AL, Bontrager MG, Ågren J (2020) What do we really know about adaptation at range edges? *Annual Review of Ecology, Evolution, and Systematics* 51:341–361.
74. Sagarin RD, Gaines SD (2002) The 'abundant centre' distribution: to what extent is it a biogeographical rule? *Ecology Letters* 5(1):137–147.
75. Martin PR, Robinson OJ, Bonier F (2024) Rare edges and abundant cores: range-wide variation in abundance in north american birds. *Proceedings of the Royal Society B* 291(2015):20231760.
76. Willi Y, et al. (2022) Conservation genetics as a management tool: The five best-supported paradigms to assist the management of threatened species. *Proceedings of the National Academy of Sciences* 119(1):e2105076119.
77. Lande R (1988) Genetics and demography in biological conservation. *Science* 241(4872):1455–1460.
78. Frankham R (2005) Genetics and extinction. *Biological conservation* 126(2):131–140.
79. Flather CH, Hayward GD, Beissinger SR, Stephens PA (2011) Minimum viable populations: is there a 'magic number'for conservation practitioners? *Trends in ecology & evolution* 26(6):307–316.
80. Jamieson IG, Allendorf FW (2012) How does the 50/500 rule apply to mvps? *Trends in ecology & evolution* 27(10):578–584.
81. Aitken SN, Whitlock MC (2013) Assisted gene flow to facilitate local adaptation to climate change. *Annual review of ecology, evolution, and systematics* 44(1):367–388.
82. Barton N, Depaulis F, Etheridge A (2002) Neutral evolution in spatially continuous populations. *Theoretical Population Biology* 61(1):31–48.
83. Lande R, Engen S, Sæther BE (2003) *Stochastic population dynamics in ecology and conservation*. (Oxford University Press, Oxford, UK).
84. Polechová J, Barton N (2005) Speciation through competition: A critical review. *Evolution* 59(6):1194–1210.

DRAFT

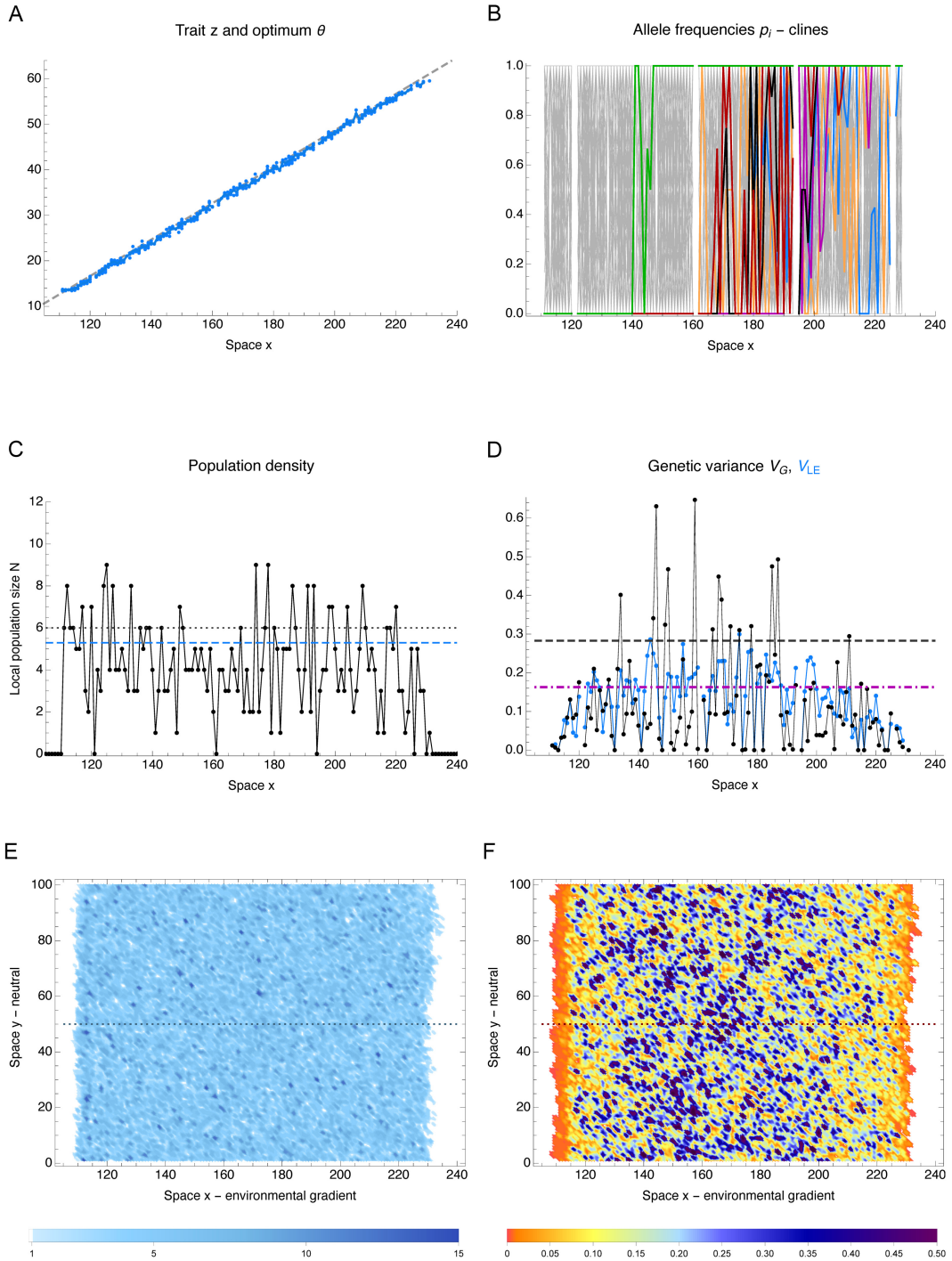

Fig. S1 Illustration of coupled evolutionary and population dynamics with slow temporal change $k^* = 0.1$ and effective spatial gradient $B = 0.2$. (A–D) transect at central neutral habitat; (E, F) two-dimensional view across the space. (A) As optimum changes slowly through time (to the left), trait mean $\overline{z}$ (blue; line: mean, dots: individuals) lags just very slightly behind the optimum θ (gray dashed line). (B) Clines which underlie the trait, are nevertheless very noisy: this is due to the combination of genetic drift and temporal change. All clines are shown as a grey background, six coloured clines give illustrate the observed cline shapes. (C) Local population size is on average close to the deterministic expectation in the absence of temporal change (red dashed line); dotted line gives the carrying capacity $K = 6$. (D) Genetic variance is even more noisy, yet the average is not far from the expected value in the presence of drift (but no temporal change), shown in dash-dotted magenta (see Fig. 2.) Dashed black line gives the expected variance in the absence of genetic drift as well as temporal change ($V_G = b\sigma\sqrt{V_s}$). Total genetic variance is shown in black, linkage equilibrium component in blue: while overall the they are close, there may be significant departures from linkage equilibrium locally. (E) Population is continuous, while local population size is around the expected value. (F) Genetic variance varies across space with an average around the expected value away from the (variation-depleted)edges. Parameters as in Fig 3, with $k^* = 0.1$. Mean neighbourhood size $\mathcal{N} = 14$, total population size $N_{tot} = 5 \cdot 10^4$.

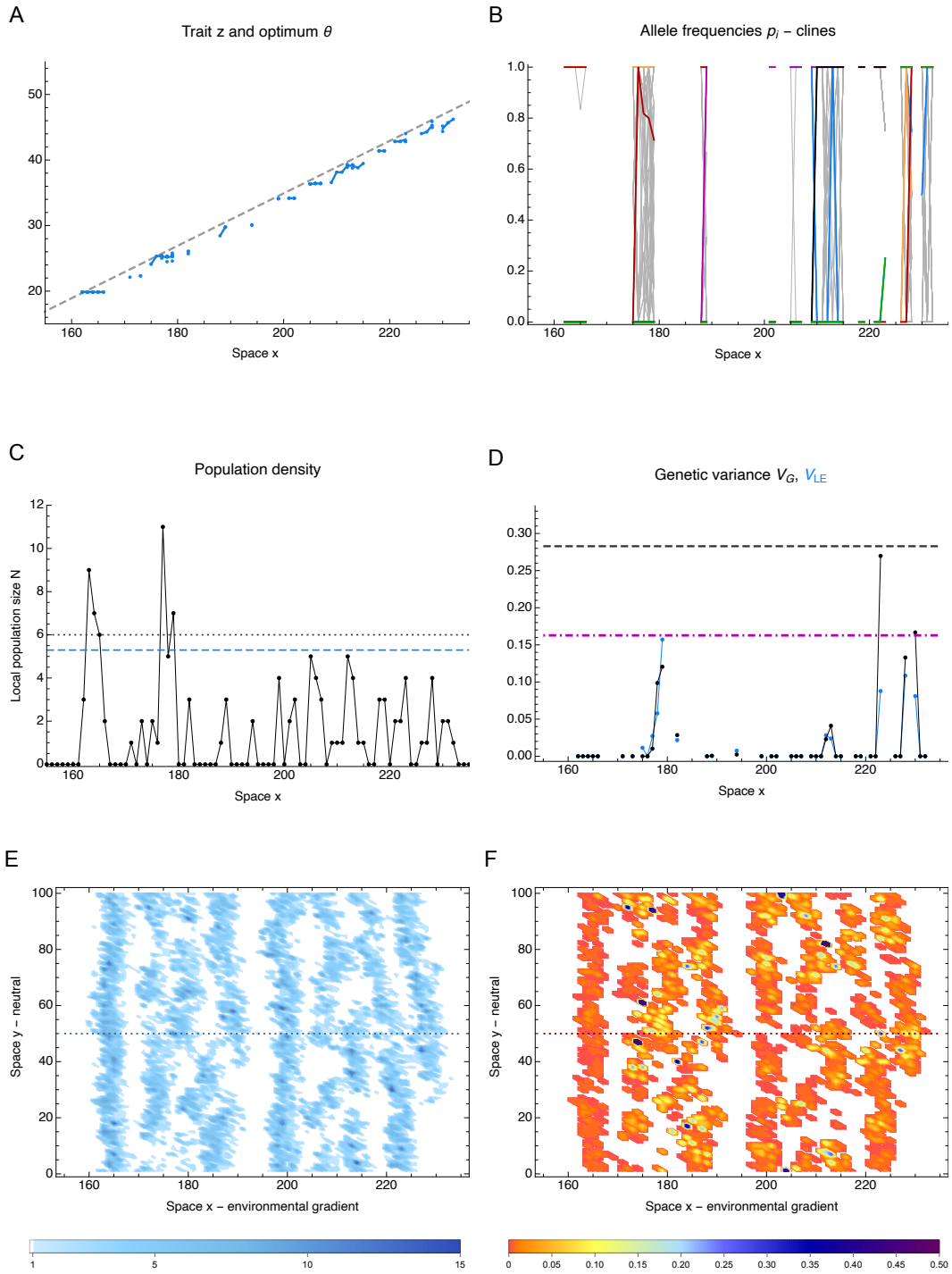

Fig. S2 Illustration of coupled evolutionary and population dynamics with fragmentation under fast temporal change $k^* = 0.26$ and effective spatial gradient $B = 0.2$. (A–D) transect at central neutral habitat; (E, F) two-dimensional view across the space. (A) As optimum changes through time (to the left), trait mean $\bar{z}$ (blue; line: mean, dots: individuals) lags behind the optimum θ (gray dashed line). (B) Clines which underlie the trait are very noisy: this is due to the combination high stochasticity under fast temporal change. All clines are shown as a grey background, six coloured clines give illustrate the observed cline shapes. (C) Local population size fluctuates substantially, as is on average considerably lower than the deterministic expectation in the absence of temporal change (red dashed line); dotted line gives the carrying capacity $K = 6$. (D) Genetic variance is depleted yet in some patches close to the expected value in the presence of drift (but no temporal change), shown in dash-dotted magenta (see Fig. 2.) Dashed black line gives the expected variance in the absence of genetic drift as well as temporal change ($V_G = b\sigma\sqrt{V_s}$). Total genetic variance is shown in black, linkage equilibrium component in blue: while overall the they are close, there may be significant departures from linkage equilibrium locally. (E) Population is highly fragmented yet still connected along the neutral habitat (y). (F) Genetic variance is mainly depleted (red), maintained only in a few small patches. Parameters as in Fig 3, with $k^* = 0.26$ above the expansion threshold $k_e^*(\mathcal{N}, B) = 0.2$. Mean neighbourhood size $\mathcal{N} = 10$, total population size $N_{tot} = 1.2 \cdot 10^4$.

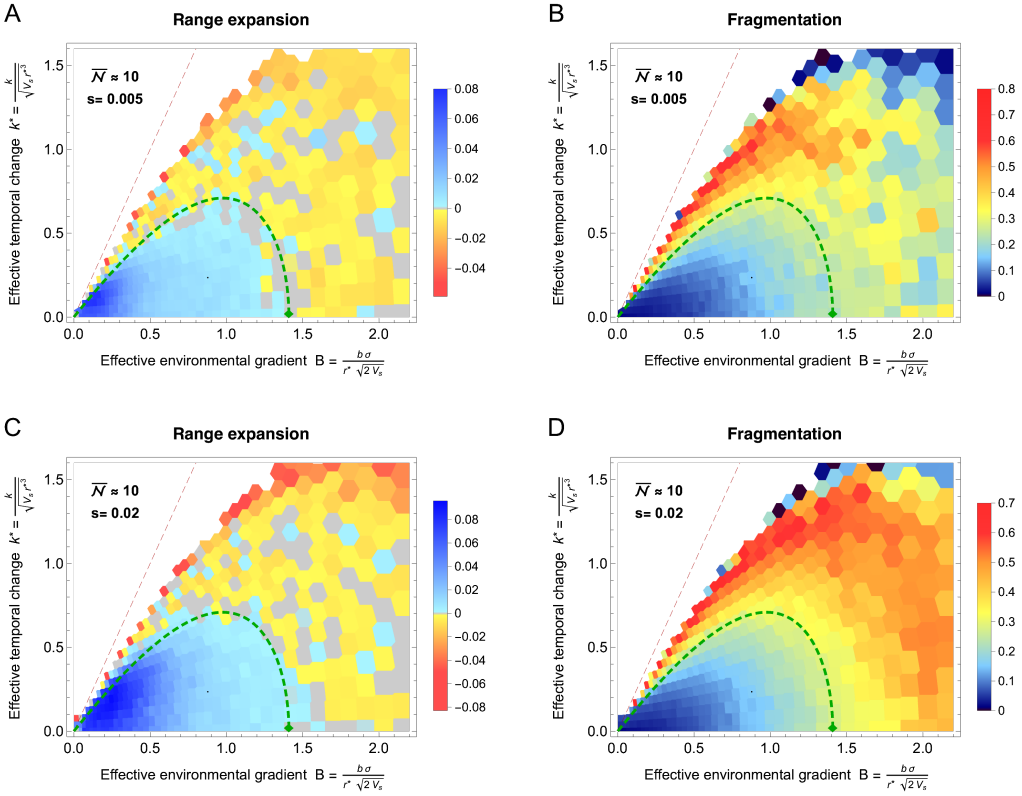

Fig. S3 The expansion threshold (dashed green curve), which describes the tension between polygenic adaptation and genetic drift, is approximately independent of the strength of selection per locus, $s \equiv \alpha^2/(2V_s)$. However, there is a tendency for selection to overcome genetic drift marginally sooner when selection per locus is stronger ((A, B) $s = 0.005$ *vs.* (C, D) $s = 0.02$). Notice that the fragmentation signal is clearer under stronger selection in (D) as stochastic extinction of subpopulations (fragments) is reduced. This is because missing fragments can result in a *lower* measured fragmentation (calculated as the proportion of unoccupied habitat) when marginal populations go extinct, and because fragmentation drops to zero when only one subpopulation remains. The negligible effect of weak selection on genetic drift in clines within continuous two-dimensional habitats is discussed in [82]. Dashed red line gives the deterministic extinction threshold. Parameters are as in Fig. 1 with allelic effects α fixed at $\alpha = 0.1$ for (A, B) and $\alpha = 0.2$ for (C, D); the number of loci scales inversely with α to 1000 and 500, respectively – ensuring comparable range sizes at time zero.

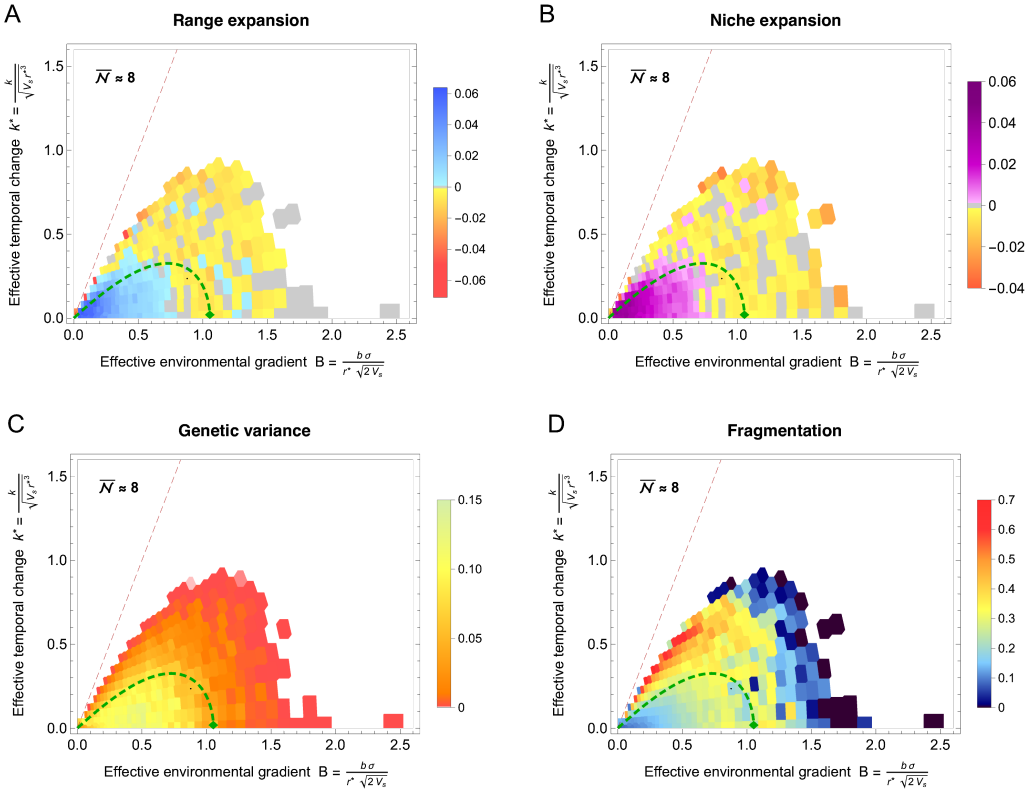

Fig. S4 Coevolution of species' range, niche and local genetic variance: low neighbourhood size. As neighbourhood size decreases, expansion threshold (dashed green curve) moves toward weaker gradients B and slower rate of temporal change k^*. It is apparent that with very low neighbourhood sizes, demographic stochasticity becomes significant and range expansion for high effective spatial gradient B ceases a little earlier than predicted. There is also a marked increase of fragmentation as B increases: the subsequent decrease in fragmentation for very steep gradients means that there is only a single surviving (but collapsing) population. For weak gradients, we see that the population expands a little beyond the approximate threshold: this is because this neighbourhood size is very low, where the approximation of reduction of genetic variance starts to diverge (the prediction gives a lower genetic variance than observed): see Fig. 2. Dashed red line gives the deterministic extinction threshold. Parameters as in Fig 1 but maximum local carrying capacity $K = 4$, the neutral habitat width is $y_d = 600/4 = 150$ This gives neighbourhood size with median $\overline{\mathcal{N}} = 2\pi\sigma^2 N \approx 8$, ranging from $\mathcal{N} = 6$ to $\mathcal{N} = 11$ and total population size with median $2.8 \cdot 10^3$ for surviving populations, ranging from 130 to $3 \cdot 10^5$ for expanding populations at $T = 500$ generations.

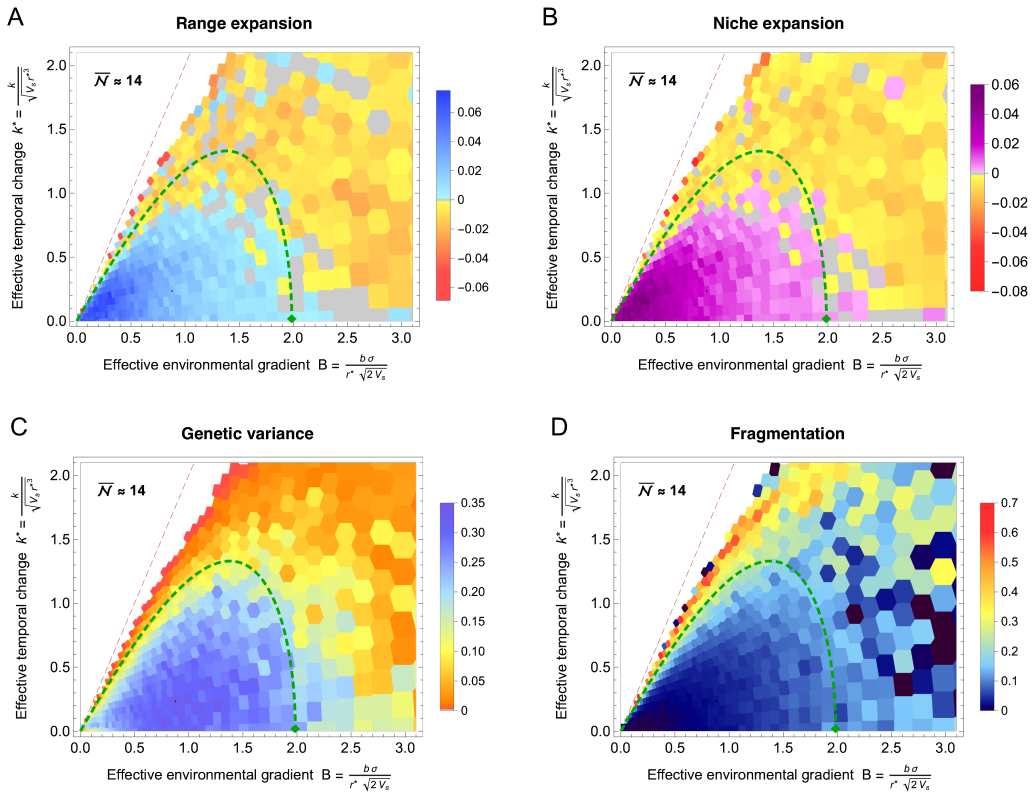

Fig. S5 Coevolution of species' range, niche and local genetic variance: larger neighbourhood size. As neighbourhood size increases, species' range and niche expands for steeper gradients B and faster rate of temporal change k^*. Under no temporal change $k^* = 0$, the positive rate of range and niche expansion extends slightly beyond the approximate the expansion threshold (dashed green curve), albeit the rates of expansion are very slow. In contrast, we see only few singular weakly expanding populations for $k^* > 0$ (some noise is expected with CI of 95% for over 1000 independent simulations). Dashed red line gives the deterministic extinction threshold. Parameters as in Fig 1 but maximum local carrying capacity $K = 10$, the neutral habitat width is $y_d = 600/10 = 60$; notice the change of scale. This gives neighbourhood size with median $\overline{\mathcal{N}} = 2\pi\sigma^2 N \approx 14$, ranging from $\mathcal{N} = 10$ to $\mathcal{N} = 30$ and total population with median $3.7 \cdot 10^3$ for surviving populations, ranging from 600 to $4 \cdot 10^5$ for expanding populations at $T = 500$ generations.

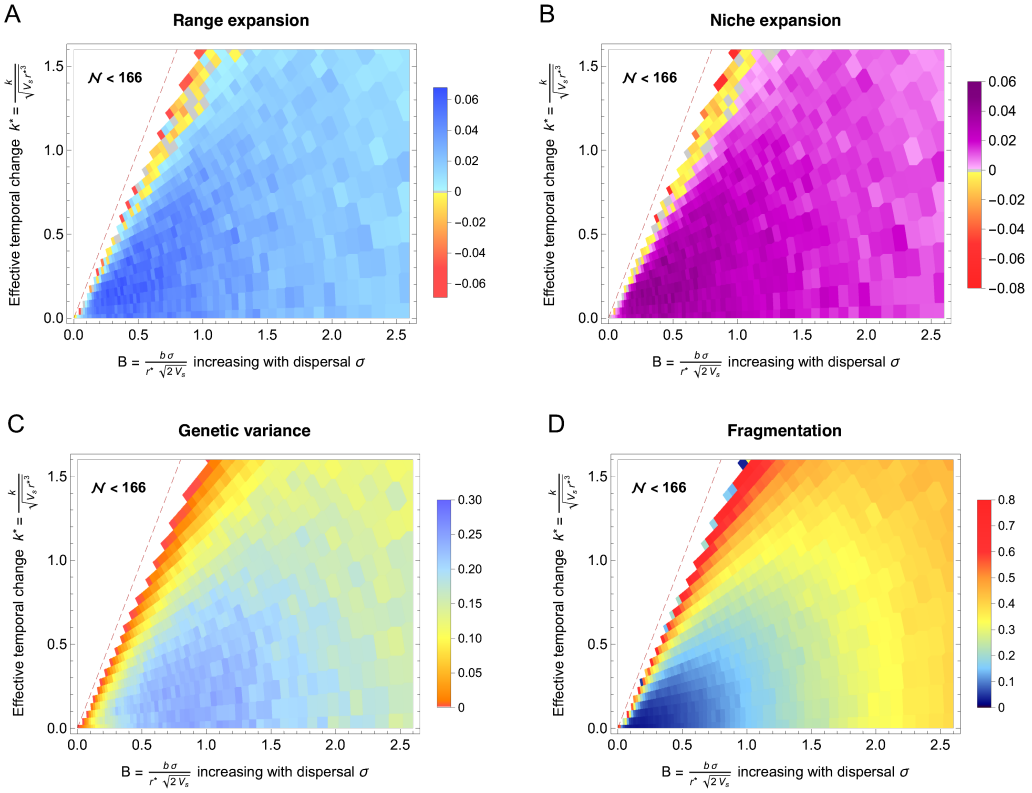

Fig. S6 Gene flow across heterogenous environments facilitates adaptation. This figure illustrates that when local population density is small, the benefits reducing genetic drift by increasing dispersal σ outweigh the costs incurred by elevated dispersal load. In contrast to Fig. 1, here the effective environmental gradient $B = b\,\sigma/(\sqrt{2V_s}\,r^*)$ increases with dispersal, which also elevates the neighbourhood size $\mathcal{N} = 2\pi\,\sigma^2\,N$. Then, the expansion threshold k_c^* (dashed green curve in previous figures) vanishes, and species' range (A) and niche (B) keeps expanding for increasing effective environmental gradient B . Yet, dispersal still carries a demographic cost. This manifests both in a gradual decline in genetic variance (C) for very steep effective environmental gradients B and in gradually increasing fragmentation (D). This is expected: eventually, the combined demographic loads (dispersal, variance and lag loads) will become too large and the population will gradually approach deterministic extinction. The deterministic extinction threshold due to high lag load is depicted by dashed red line. Parameters as in Fig 1 but with B increasing with dispersal distance σ, ranging from 0.1 to 3.5, and $\mathcal{N}$ ranging from 1 to 166 (median $\mathcal{N} = 65$), while the local carrying capacity stays at $K = 6$. The median total population was around $1.4 \cdot 10^4$ for surviving populations, ranging from 2630 to $4.4 \cdot 10^5$ for expanding populations at $T = 500$ generations.

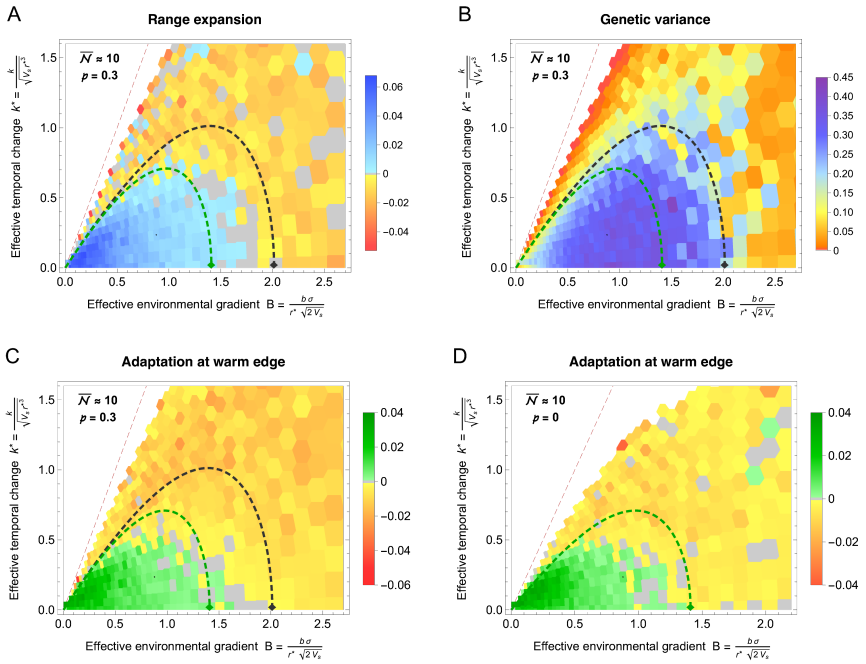

Fig. S7 Adaptive phenotypic plasticity facilitates adaptation to spatial but not temporal change when genetic variance is maintained by migration-mutation-selection balance. (A) Species' range continues to expand under steeper effective environmental gradients B in the presence of adaptive phenotypic plasticity $\mathfrak{p}$. This is depicted by the dashed black curve, while the reference without plasticity (as in Fig. 1) is shown in green. (B) Genetic variance is maintained for higher B since the impact of the environmental gradient on fitness, and the associated increase in genetic drift, is reduced. However, the limiting temporal change k_e^* for a given gradient B, beyond which adaptation ceases, does not change significantly due to plasticity. This occurs because adaptive plasticity $\mathfrak{p}$ weakens effective selection, thereby reducing the extent to which genetic variance, essential for adaptation to temporal change, increases with the spatial gradient. At the deterministic limit, variance will be reduced by a factor of $(1-\mathfrak{p})$, hence the effect of phenotypic plasticity cancels. (C) The rate of adaptation at the *warm* edge (i.e., in the direction of temporal change in the optimum) improves only marginally due to plasticity, and only when the spatial gradient B is steep and the rate of temporal change k^* is slow. (D) The rate of adaptation in the absence of plasticity is similar but shows noticeably higher noise due to greater demographic stochasticity. Parameters are as in Fig. 1, except for plasticity, which is set to $\mathfrak{p} = 0.3$ in (A–C). Median neighbourhood size $\overline{N} = 2\pi\sigma^2 N \approx 10$ ranges from 8 to 17, and is higher for lower B and k^*, where the overall demographic load is lower. Median total population size is approximately $4 \cdot 10^3$ for all surviving populations, ranging from 640 to $3.2 \cdot 10^5$ for expanding populations at $T = 500$ generations.